The anharmonic infrared spectra of polycyclic aromatic hydrocarbons

Mackie, J.C.

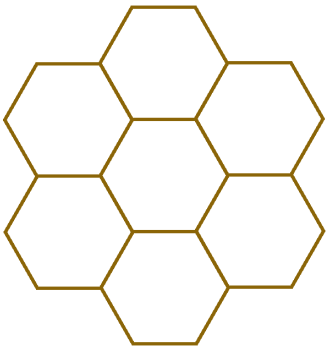

Fully anharmonic infrared cascade spectrum of polycyclic aromatic hydrocarbons

The infrared (IR) emissions of polycyclic aromatic hydrocarbons (PAHs) permeate our universe; astronomers have detected the infrared signature of PAHs around every interstellar object with sufficient energy to excite them. The IR emission of interstellar PAHs differs from their emission seen under conditions on Earth, as they emit through a collisionless cascade down through their excited vibrational states from high internal energies. The difficulty in reproducing interstellar conditions in the laboratory results in a reliance on theoretical techniques. However, the size and complexity of PAHs requires careful consideration when producing the theoretical spectra. In this work we outline the theoretical methods necessary to lead to a fully theoretical IR cascade spectra of PAHs including: an anharmonic second order vibrational perturbation theory (VPT2) treatment; the inclusion of Fermi resonances through polyads; and the calculation of anharmonic temperature band shifts and broadenings (including resonances) through a Wang–Landau approach. We also suggest a simplified scheme to calculate vibrational emission spectra that retains the essential characteristics of the full IR cascade treatment and can directly transform low temperature absorption spectra in IR cascade spectra. Additionally we show that past astronomical models were in error in assuming a 15 cm^{-1} correction was needed to account for anharmonic emission effects.

C. J. Mackie, T. Chen, A. Candian, X. Huang, T. J. Lee, and A. G. G. M. Tielens, Submitted (2018)

7.1 Introduction

Polycyclic aromatic hydrocarbons (PAHs) are a family of molecules characterized by containing multiple fuzed benzenoid rings with the free edges capped with hydrogen. Their size, complexity, stability, and universal abundance make their study appealing to vastly different areas of research: from biology for their carcinogenic properties[3], to material science for their desirable structural properties[5, 6, 7], to engineering for their role in the undesirable combustion byproducts of engines and rockets[2]. Perhaps the most surprising field to study PAHs is astronomy. The infrared (IR) signatures of aromatic carbon–containing molecules have been observed in all interstellar objects with sufficient ultra–violet (UV) radiation to excite them; from reflection nebulae, to photo–dissociation regions, to emissions from distant galaxies as a whole[78]. These so–called "aromatic infrared bands" (AIBs) are generally attributed to PAHs and PAH derivatives[29, 30]. The interstellar PAHs absorb UV photons from a source (i.e., a parent star) becoming electronically excited, then quickly (hundreds of femtoseconds) return to their electronic ground state through emission-less internal conversion into highly excited vibrational states. They then relax radiatively through gradual (˜seconds) emission of IR photons from their excited vibrational states producing what is known as an *IR cascade spectrum*[41, 103].

Producing experimental IR cascade spectra under astrophysically relevant conditions (i.e., an extreme vacuum with zero collisions) is extremely difficult with current technologies. Therefore, extrapolations from available data must be made. Experimental high–resolution, low–temperature, gas–phase emission spectra would be ideal. However, experiments have been limited largely to either high–temperature gas–phase absorption spectra[21, 81, 82], or low–temperature matrix–isolation spectra[22, 23, 24, 79, 108, 109]. The usefulness of these experiments in modeling IR cascade spectra are complicated by temperature and pressure effects in the former, and unpredictable matrix interaction effects in the later. Recently, high–resolution, low–temperature, gas–phase *absorption* spectra have been produced for a handful of small PAH species in the CH–stretching IR region[25, 26, 27].

Due to the large variety and size of PAHs, most theoretical calculations to date have been performed using low levels of theory, typically scaled density functional theory (DFT) calculations at the double harmonic level, using the B3LYP functional[126] and 4-31G[140] basis set. Databases of the theoretical calculations of PAHs have been compiled[36, 50] and are used by astronomers in modeling PAH IR cascade emission. These databases have been vital to understanding the variation in the PAH emission observed both between different interstellar environments, and spatially within a given interstellar object. These variations can be used to track properties such as size, structure, temperature, and charge balance[18, 28, 33].

Although successful in many ways, detailed comparison between theory and experiments have revealed that that these double harmonic calculations cannot model accurately the PAH emission at high resolution, especially in the CH–stretching region centered around 3.3 μm[25, 26, 27]. While this has not hindered observations of PAHs using current telescopes, it is bound to become a glaring issue with the

upcoming launch of the James Webb Space Telescope, which will give an unprecedented combination of spectral and spatial resolution in the infrared region. Recent work has shown[105, 125, 132] that in order to overcome these deficiencies an anharmonic approach is necessary. The anharmonic approach is not only better in predicting the vibrational fundamental band positions and intensities themselves, but also allows for the calculation of combination bands, overtones, and hot–bands. Additionally, anharmonic calculations can account for mixing between modes in *Fermi resonances*, which are vitally important for reproducing the 3.3 μm region accurately.

These anharmonic calculations also allow for an ab–initio approach for generating internal energy/temperature dependent spectra. Two main methods have been put forward: a direct approach – whereby the thermal population of each vibrational state is calculated, then transition energies and intensities are calculated for every possible transition between populated states[84]; and a statistical approach – whereby a biased Monte Carlo walk, known as the Wang–Landau method[134, 135], is used to construct the density of states (DoS) and the energy dependent spectra. These methods then produce temperature dependent spectra through a Laplace transformation[133]. This latter approach has been shown to be quite efficient since the time consuming DoS and energy spectrum calculations need to be performed only once for each molecule, then any desired temperature spectrum can be generated in a matter of seconds using the Laplace transformation. The latter method has also been shown to be advantageous in that incorporating the important Fermi resonances into the spectrum is a straight forward exercise[141].

The collision–free cascade emission process of PAHs needs to be considered when modelling the IR spectrum of interstellar PAHs. As stated previously, the PAHs absorb UV photons, interconvert electronically into the ground electronic state with excited vibrational states, then emit IR photons slowly as they cool. Attempts have been made to replicate these conditions in the laboratory[42, 43, 44] with some success. Theoretical modelling of the IR cascade emission has also been performed, typically using DFT calculations at the double harmonic level[45, 46], and to a lesser extent at the anharmonic level[137, 138]. However, a sufficient treatment of Fermi resonances in a full anharmonic cascade model has never been taken into account previously, leading to spectra that could not be fully trusted, especially in the troublesome 3.3 μm region. Additionally, due to the limited datasets and number of species analyzed, these previous studies have given rise to approximated methods whose validity has to be assessed, as will be explained below.

With the proper incorporation of anharmonicities, resonances, and internal energy/temperature dependence (including the incorporation of polyads), the ingredients are present for a full theoretical anharmonic IR cascade spectra of PAHs. In this work, these calculations are performed for a small subset of astrophysically relevant species, including regular, hydrogenated, and methylated PAHs, as well as cationic species (see supporting material for all results). This work also shows that the Wang–Landau approach can reach the same accuracy of more "exact" techniques like the direct counting methods at a fraction of the computational

cost. The indivual theories underlying each theoretical step used towards the full cascade model are outlined in section 7.2. Details of the application of these methods are given in section 7.3. The results are give in section 7.4 as well as in the supporting material. Discussion and conclusions follow.

7.2 Theory

7.2.1 Anharmonicity

In the double harmonic approximation the vibrational potential of a molecule in its stationary point geometry is given by

$$V = \frac{1}{2} \sum_{i=1}^{3N} \sum_{j=1}^{i} F_{ij} X_i X_j \tag{7.1}$$

where V is the total vibrational potential, $F_{ij} = \frac{\partial V}{\partial X_i \partial X_j}$ are the quadratic force constants between atoms i and j, and X_i and X_j are the Cartesian coordinates of atom i and j relative to the stationary point geometry.

The quadratic force constants are computed through ab–initio analytical second derivative techniques. Once computed these quadratic force constants are used to construct a Hessian matrix, which upon diagonalization yields the individual vibrational band energies (harmonic frequencies) as the eigenvalues, and the individual vibrational mode displacement descriptions or "normal modes" as the eigenvectors. This method results in 3N-6 normal modes for non–linear molecules and 3N-5 normal modes for linear molecules (where N is the number of atoms). The harmonic intensities of the vibrational modes are calculated using the double harmonic approximation, whereby a matrix is constructed and solved using the derivatives of the dipole moment as the molecule is displaced along its normal modes. In this approximation the intensities of the overtones, combinations bands, and hot bands are exactly zero. Additionally, interactions between modes such as couplings and resonances cannot be taken into account. This results in a spectrum that needs to be scaled in frequency, and a spectrum that miss a large number of features. In addition this, in order to include temperature effects such as band broadenings and shifts empirically derived expressions need to be applied[45, 47].

To account for these short comings, a more accurate approach is necessary. Ideally, the exact potential could be written as an infinite order Taylor series. The harmonic equation above would represent the first order terms of such an expansion. Subsequent higher order terms would include cubic, quartic, pentic, hextic, etc. force constants (derivative terms). However, to sufficiently account for combination bands, overtones, hot–bands, couplings, resonances, and temperature effects it is enough to include the first three non–zero terms of the expansion,

leading to the so–called anharmonic quartic force field (QFF)

$$\begin{aligned} V = & \frac{1}{2}\sum_{i=1}^{3N}\sum_{j=1}^{i}\left(\frac{\partial^2 V}{\partial X_i \partial X_j}\right)_{V_0} X_i X_j \\ & + \frac{1}{6}\sum_{i=1}^{3N}\sum_{j=1}^{i}\sum_{k=1}^{j}\left(\frac{\partial^3 V}{\partial X_i \partial X_j \partial X_k}\right)_{V_0} X_i X_j X_k \\ & + \frac{1}{24}\sum_{i=1}^{3N}\sum_{j=1}^{i}\sum_{k=1}^{j}\sum_{l=1}^{k}\left(\frac{\partial^4 V}{\partial X_i \partial X_j \partial X_k \partial X_l}\right)_{V_0} X_i X_j X_k X_l \end{aligned} \tag{7.2}$$

A simple Hessian can no longer be constructed to solve this potential since it is now non–linear. Instead, the harmonic solution is calculated as usual, then the cubic and quartic force constants are used to perturb the harmonic solution in a second order perturbation theory treatment (VPT2) (see Ref. [86] for a full description). With the total vibrational energy of the perturbed molecule given by

$$\begin{aligned} E(v) = & \sum_k \omega_k \left(n_k + \frac{1}{2}\right) + \sum_{k\leq l} \chi_{kl}\left(n_k + \frac{1}{2}\right) \\ & \times \left(n_l + \frac{1}{2}\right) \end{aligned} \tag{7.3}$$

where ω_k is the harmonic frequency of the k^{th} fundamental, n_k are the number of quanta in the k^{th} fundamental vibrational mode, and χ_{kl} are the corresponding anharmonic constants, with the anharmonic constants being calculated from the cubic and quartic force constants (see 87). Combination bands are given as the sum of the perturbed fundamentals, and the hot–bands and overtones are determined by increasing the number of quanta in the relevant vibrational modes. Equation 7.3 shows that the vibrational band positions are no longer independent, but now depend on the excitement of the other vibrational modes. This gives rise to temperature dependent shifts and broadenings, which will be expanded upon below.

Intensities can also be calculated at the anharmonic level for fundamentals, overtones, and combination bands. See Ref. 90 for the complete set of equations.

Figure 7.1 shows the effect that including anharmonicities into the potential energy surface has on the infrared spectrum of a PAH. A comparison is made between the unshifted harmonic, full anharmonic, and high–resolution low–temperature gas–phase experimental[27] infrared spectrum of the 3.3 μm CH–stretching region of 9-methylanthracene. This region is particularly sensitive to anharmonic effects.

7.2.2 Resonances and polyads

In an anharmonic treatment the vibrational modes are no longer independent from one another, and so they can interact through *resonances*. A resonance occurs when the energy of the normal modes or the sum of modes are close to one

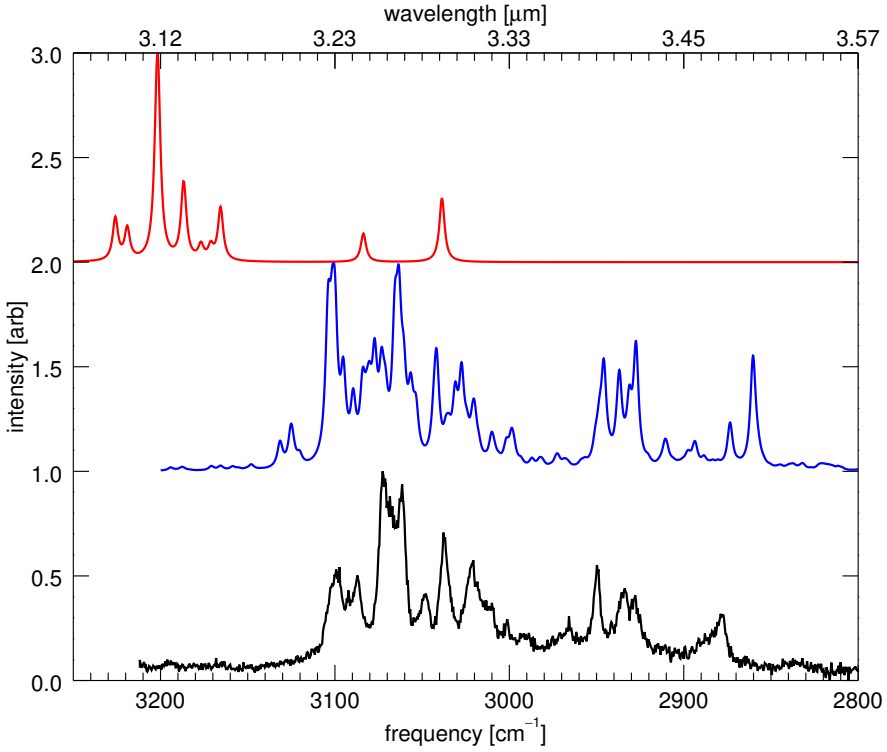

Figure 7.1 The change in the theoretical infrared spectrum of 9-methylanthracene when moving from a harmonic (red) to anharmonic (blue) treatment compared to high–resolution low–temperature gas–phase experimental[27] spectrum (black).

another in energy. Mathematically speaking, a resonance occurs in the context of a VPT2 treatment when the denominator of a term in the anharmonic constant calculation approaches zero causing the offending term to increase dramatically in value. These singularities or resonances have to be removed from the VPT2 treatment and handled separately in a method akin to second order degenerate perturbation theory (see reference 51 and references therein). In a typical VPT2 treatment four main types of resonance occur: Coriolis, when two fundamental vibrational modes are approximately equal to one another; Darling–Dennison, when two vibrational first overtones are approximately equal to one another; type one Fermi, when one fundamental vibrational mode is approximately equal to a first overtone; and type two Fermi, when one fundamental vibrational mode is equal to the sum of two vibrational modes. The result of a resonance on a spectrum is that the vibrational modes involved tend to push one another apart in frequency (compared to their non–resonant frequencies) and their intensities can be redistributed between them.

Complicating matters further is that any given vibrational state can be involved in many different resonances simultaneously. It is not sufficient to handle each resonance individually, instead these groups of mutually resonating modes or *polyads* need to be handled variationally through the construction of a resonance matrix. The diagonal terms of this matrix are the perturbed states as given in equation 7.3 (with the resonant terms already removed from the anharmonic constants) and the off diagonal terms are the coupling constants (see reference 58 for more details). Diagonalization of this matrix gives the new line positions as the eigenvalues, and the strengths of the state mixings as the square of the eigenvectors. These state mixing terms can be used to determine the redistribution of intensities between resonating modes[105]. This treatment was applied to a series of PAHs in our previous works[105, 125, 132] and was shown to be crucial in reproducing the CH–stretching region due to the large number of type two Fermi resonances.

Figure 7.2 shows the effect of performing a polyad resonance treatment on the 0 Kelvin anharmonic infrared spectrum of a 9-methylanthracene. A comparison is made between the convolved (HWHM = 1.8 cm^{-1}) anharmonic spectrum with the polyads suppressed, with the polyads included (the same as figure 7.1), and the high–resolution low–temperature gas–phase experimental[27] infrared spectrum of the 3.3 μm CH–stretching region.

7.2.3 Temperature dependent spectra

Detailed models describing the temperature effects on IR spectra of PAHs have been pioneered by references 84, 133, 136, 137, 139. Here, we summarize their approach for completeness. The first step in producing a temperature dependent spectrum is to calculate the vibrational DoS (Ω). As the number of atoms in a molecule increases, the number of possible states falling in a given energy range grows extremely fast, especially at high internal energies. For this reason exact counting of the density of states becomes impossible. Therefore, Monte Carlo type samplings are used instead, with the preferred method for calculating the DoS being the Wang–Landau method[134, 135]. Producing temperature–dependent

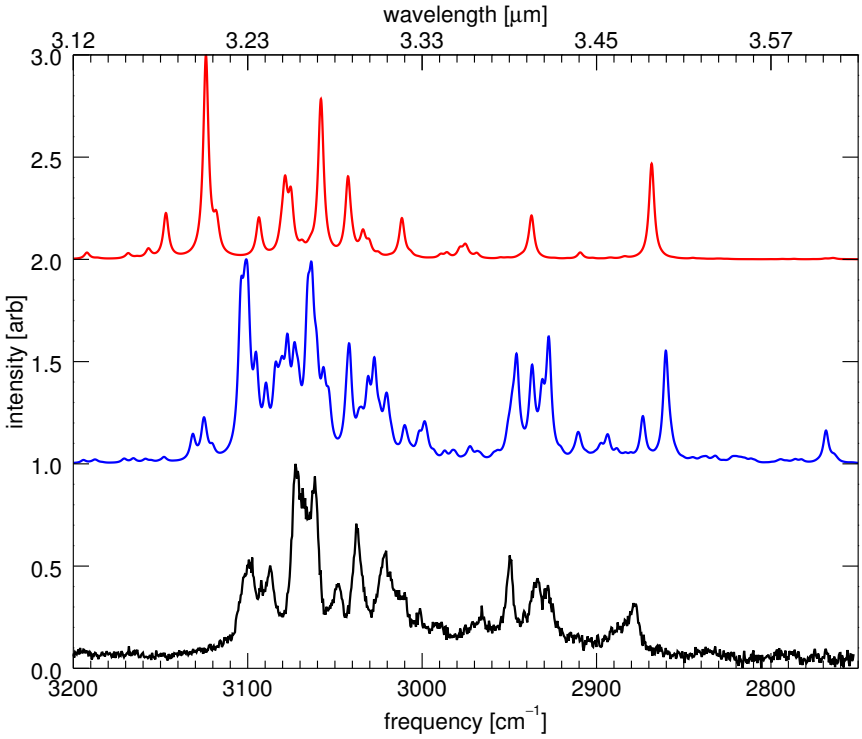

Figure 7.2 The change in the 0 K theoretical infrared spectrum of 9-methylanthracene when moving from a non–polyad treatment (red) to a polyad treatment (blue) compared to high–resolution low–temperature gas–phase experimental[27] spectrum (black).

spectra from a QFF using a Wang–Landau style walk has been shown previously to work successfully for PAHs[133, 136], therefore similar methods have been adopted in this work.

The aim of a Wang–Landau walk is to visit all predefined energy bins (δE) equally in an efficient manner. This is accomplished by biasing the walk to prefer states that have been visited less than the energy bin of the current state. Initially, Ω is set to 1 for the whole energy range of interest ($[E_{min},E_{max}]$). The set of vibrational quantum numbers {n} is initially set to a random state inside the energy range. At each step there is a probability that any of the vibrational quantum numbers can either increase or decrease by one quanta, or remain the same. The value of this probability is chosen to be large enough so that the walk covers the whole energy range in a reasonable amount of steps, but also small enough as to not jump outside of the energy range constantly. Typical values for this probability range from 4–23%. After the set of new quantum numbers, $\{n\}_{new}$, are generated the probability (P) that this state is accepted into the accumulation of Ω is given by

$$P(\{n\}_{current} \rightarrow \{n\}_{new}) = min[1, \frac{\Omega(E_{current})}{\Omega(E_{new})}] \tag{7.4}$$

If the new state is accepted then $\Omega(E_{new})$ is updated by adding a quantity f, where f is a modification factor set to some initial quantity greater than zero (typically the mathematical constant e). Since Ω can become quite large, the value $\ln(\Omega)$ is generally stored instead. A histogram of number of times a energy bin is visited is also accumulated to test for equal sampling (flatness) of the walk. After sufficient flatness is achieved, the value of f is updated by taking its square root, H is reset, and the walk is continued again until the flatness is once again achieved. This process of updating f and re–running the walk ensures quick and accurate convergence towards the true DoS. Typically, f is updated and the walk re–run on the order of 20 times, depending on the desired accuracy of the density of state calculation.

Once Ω is calculated, the next step is to produce the absorption spectrum of the molecule. A separate Wang–Landau walk over the same internal energy range is performed. With the acceptance criteria of a state (P) now being based on the completed Ω(E) values.

At each step of this second walk an accumulated absorption spectrum $\mathcal{S}$ at internal vibrational energy E is updated according to

$$\mathcal{S}(\nu, E) = \sum_k (n_k + 1)\sigma_{0\rightarrow 1}^{(k)} \delta[h\nu - \Delta E^{(k)}] \tag{7.5}$$

with $\sigma_{0\rightarrow 1}^{(k)}$ being the absorption cross section of mode k or combination band at the vibrational ground state. For combination bands n_k is taken to be the smaller of the two vibrational quantum numbers of the two bands involved.

The energy difference at the anharmonic level for a given vibrational transition

of mode k ($n_k \rightarrow n_k + 1$) is then given by

$$\Delta E^{(k)}(\{n\}) = \omega_k + 2\chi_{kk}(n_k + 1) + \frac{1}{2}\sum_{i \neq k}\chi_{ik} + \sum_{i \neq k}\chi_{ik}n_i \tag{7.6}$$

Once the walk is complete, the states are then normalized by the number of entries in the histogram giving the microcanonical absorption intensity I(ν,E).

The conversion from an energy dependent spectrum to a temperature dependent spectrum at any temperature T is then given by a Laplace transformation

$$I(\nu, T) = \frac{1}{Z(T)}\int_{E_{min}}^{E_{max}} I(\nu, E)\Omega(E)e^{(-E/k_BT)}dE \tag{7.7}$$

With Z being the partition function

$$Z(T) = \int \Omega(E)e^{(-E/k_BT)}dE \tag{7.8}$$

The maximum and minimum reliable T values are determined by the energy range of Ω. $\Omega(E)e^{(-E/k_BT)}$ at a given T should die off rapidly at E_{min} and E_{max} to ensure the integral over E_{min} to E_{max} is close to the true integral over an infinite energy range.

Figure 7.3 shows the effect of incorporating anharmonic temperature effects into the theoretical spectrum using the Wang–Landau approach. The strongest IR band of 9-methylanthracene is shown at three temperatures: 100 K, 500 K, and 1000 K. Notice the shift in band position and asymmetric broadening of the profile.

7.2.4 Polyads and temperature dependence

The incorporation of polyads into a Wang–Landau treatment of the IR energy/temperature dependent spectrum is straight forward and is outlined in reference 141. In brief, at each iteration of the Wang–Landau absorption spectrum walk a resonance matrix is constructed using the ground state resonance matrix with the diagonal terms updated by the new deperturbed transition energies given by equation 7.6, or in the case of combination bands and overtones the sum of the transition energies of the modes involved. The off–diagonal coupling terms of the resonance matrix are left unchanged as they do not depend on the vibrational energy levels occupied, but only the change in the occupation of vibrational levels of the transitions ($\Delta(n_k)$ is always 1). Once modified, the eigenvalues of the altered resonance matrix give the new transition energies of the vibrationally excited states (i.e., a new set of $\Delta E^{(k)}(\{n\})$, and the squared eigenvalues give the intensity sharing percentages over the resonating modes (i.e., a new set of $\sigma^{(k)}_{0\rightarrow 1}$). All other steps during the Wang–Landau creation of the temperature dependent spectrum remain the same[133].

Figure 7.4 shows the effect of incorporating polyads into the Wang–Landau calculations of the temperature dependent spectrum. The two spectra are of the theoretical calculations of 9-methylanthracene at 1000 Kelvin. The top spectrum

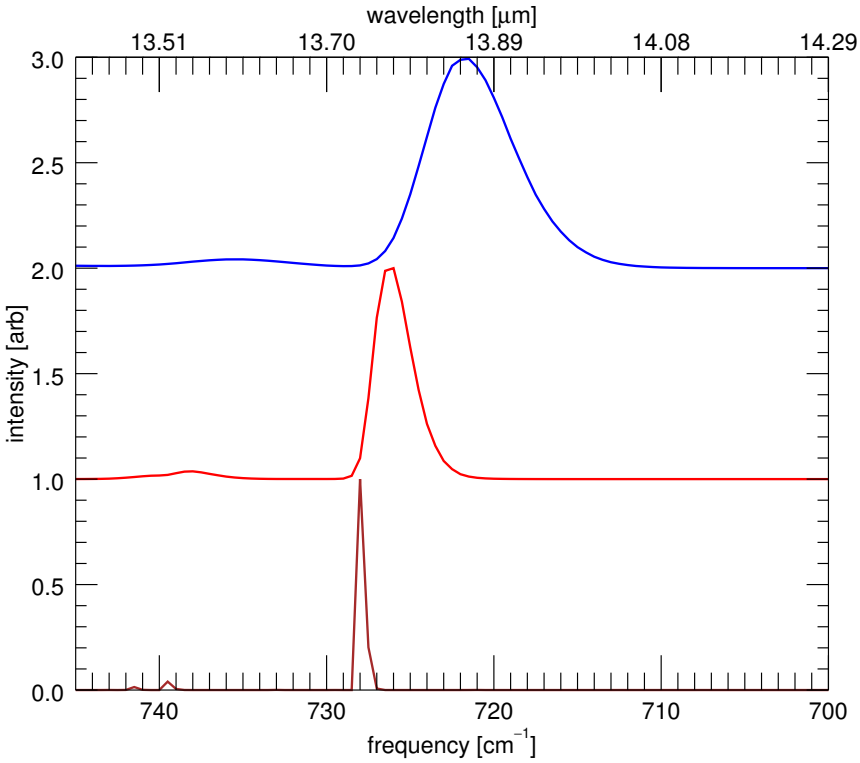

Figure 7.3 Temperature effects on the position and profile of the CH out–of–plane bending mode of the anharmonic theoretical IR spectrum of 9-methylanthracene at 100 K (brown, bottom panel), 500 K (red, middle panel), 1000 K (blue, top panel).

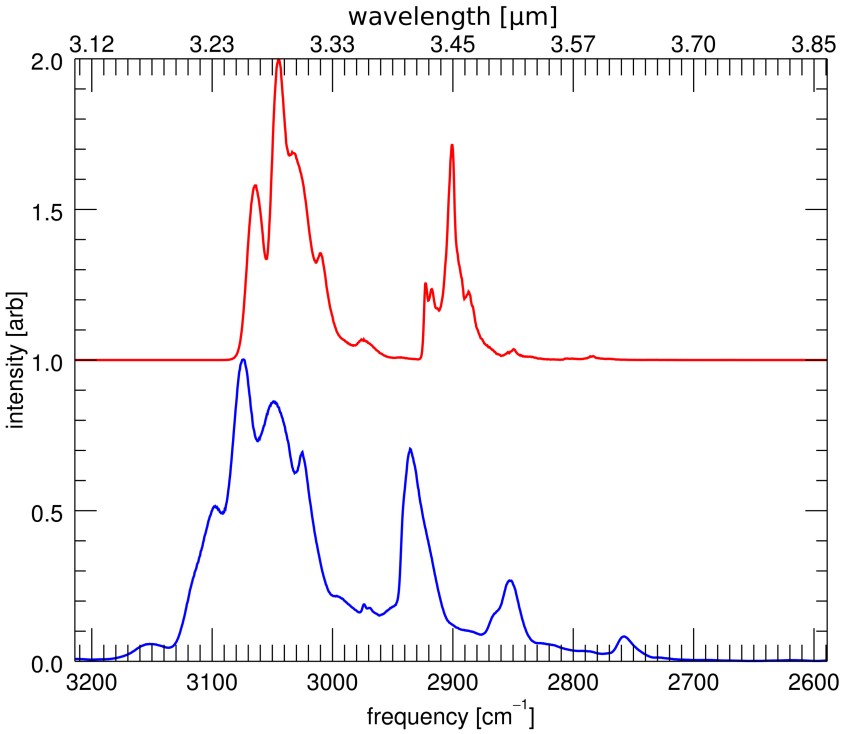

Figure 7.4 The effect of including polyads (blue, bottom panel) and excluding polyads (red, top panel) from the anharmonic temperature dependent calculations of 9–methylanthracene using the Wang–Landau approach.

(red) is the temperature spectrum with polyads suppressed, the bottom spectrum (blue) is the temperature spectrum with polyads included. Even with the line blending which occurs at high temperatures, significant issues with the polyad suppressed spectrum can still be seen. Discrepancies in band positions and widths, and the loss of features are all present when polyads are excluded.

7.2.5 PAH IR cascade spectra

Interstellar PAHs are electronically excited by UV photons originating from stellar sources, then converts quickly to their ground electronic state through emissionless internal conversion to highly excited vibrational states. PAHs then slowly emit this vibrational energy as IR radiation. When a PAH emits an IR photon, its internal energy is decreased by the energy of said photon. This decrease in internal energy affects the energy at which the next IR photons emit (see equation 7.6). In the interstellar medium this process is stochastic, in that the PAHs have time to cool

fully to the vibrational ground states in between UV photon absorption events, and collisionless, in that the only way to shed energy is through the emission of IR photons.

Modelling this process is straight forward[45]. The probability of a PAH absorbing a stellar UV photon is proportional to the product of the blackbody spectrum of a star of a given temperature and the UV absorption cross section of the PAH. The total internal vibrational energy E_{tot} of the PAH is then equal to the energy of the absorbed UV photon. The probability of emitting an IR photon (E_{IR}) at a given internal energy (E_{tot}) is proportional to its rate, which in turn is proportional to the energy dependent *emission* spectrum at E_{tot} times the square of the corresponding frequencies. Note: minor changes to equations 7.5 and 7.6 are necessary to account for emission transitions ($n_k \rightarrow n_k - 1$) rather than absorption transitions ($n_k \rightarrow n_k + 1$). Specifically, $(n_k + 1)$ terms are replace with (n_k), and $\sigma^{(k)}_{0\rightarrow 1}$ terms are replaced with $\sigma^{(k)}_{1\rightarrow 0}$. For the cascade model, an IR photon is randomly selected based on these probabilities. At each step of a cascade, a spectral histogram is updated at E_{IR}. The total internal energy is then updated: $E_{tot_{new}} = E_{tot}$ - E_{IR} leading to a new set of probabilities of IR emission. This cascade process is repeated until the PAH has fully cooled to its vibrational ground state. At this point a new UV photon is absorbed and the full cascade is repeated again. This process continues until the desired resolution is achieved.

Figure 7.5 shows a full anharmonic cascade spectrum of 9–methylanthracene pumped by an 18000 Kelvin blackbody source (simulating an OB type star). Most notable are the long red wings compared to a strictly temperature dependent spectrum as shown in Figure 7.4.

7.3 Implementation

7.3.1 Quartic force fields

The QFFs of the PAHs in this work were calculated using Gaussian 09[53] within the DFT framework, using the B3LYP functional[126] and the N07D basis set[128]. A tight convergence criterion was used for the geometry optimization and a very fine grid (Int=200974) was used for numerical integrations.

7.3.2 VPT2

The VPT2 treatment was handled by a locally modified version of SPECTRO[54], after conversion of the QFF produced by Gaussian09 from normal coordinates to Cartesian coordinates[97]. SPECTRO has the flexibility to handle large polyads as described in section 7.3.3. Additionally, the SPECTRO output of the resonant matrices were necessary for the energy/temperature incorporation as described in section 7.2.4.

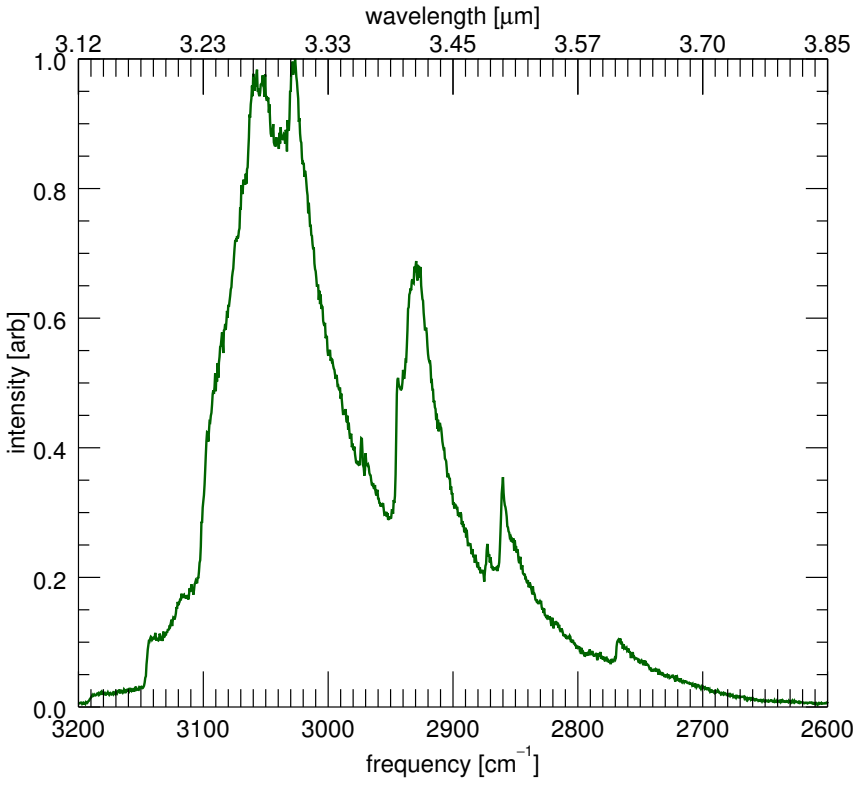

Figure 7.5 Fully anharmonic simulated cascade spectrum of the CH–stretching region of 9–methylanthracene.

7.3.3 Polyads

The cut–off for considering states to be in resonance is controlled by two parameters in SPECTRO, the minimum interaction strength between the two bands (W), and the difference in energy between the two bands (Δ). It was found[125] that the default value of W (10 cm^{-1}) missed important resonances, so this value was dropped to 0 cm^{-1}. With this value set to zero, the polyads were no longer atomically separated by irreducible representations, therefore to reduce computational cost they were separated outside of SPECTRO. The default value of Δ (200 cm^{-1}) has been shown to reproduce the CH–stretching region of PAHs accurately[125, 132]. However, polyad sizes can grow quite large with this cut–off, especially when the molecule has a low symmetry. For example, the three IR active polyads of benz[a]anthracene ($C_{18}H_{12}$, C_s symmetry) contain 117, 675, and 204 states respectively. This occurs because of *resonance chaining*, where a series of modes resonate with their neighbors who in turn resonate with their neighbors etc., leading to a polyad where the highest energy mode and the lowest energy mode could end up with a Δ that is over 1500 cm^{-1}. While diagonalizing these large polyad matrices are not a problem when obtaining a zero Kelvin vibrational spectra, they pose a significant issue when calculating an energy/temperature dependent spectra as they have to be rediagonalized with each iteration of the Wang–Landau walk. To resolve this, two separate Δ values were set: for modes > 2000 cm^{-1} Δ = 200 cm^{-1}, and for modes < 2000 cm^{-1} Δ = 25 cm^{-1}. It was found that the CH–stretching region (above 3000 cm^{-1}) is extremely sensitive to the lowering of Δ due to strong Fermi resonances and was thus left alone. Fortunately, a natural large break occurs between the CH–stretching vibrational mode energies and all other vibration modes (below 2000 cm^{-1}) so no resonance chaining occurs to the lower modes here. The vibrational modes below 2000 cm^{-1} were found to only weakly interact through Fermi resonances, so lowering Δ down to 25 cm^{-1} showed little effect on the resulting spectra, but reduced the polyad sizes dramatically.

7.3.4 Wang–Landau

For all Wang–Landau calculations the vibrational quantum number probability increase/decrease parameter was set to 5%. For the density of states calculation the energy bins were set to 25 cm^{-1}. The energy range over which the walks took place was 0–15 eV (0–120,983cm^{-1}). Twenty Wang–Landau iterations of decreasing f were run for each molecule, with each iteration consisting of 1×10^7 steps. For the majority of the energy dependent spectra the accumulated spectrum bins were set to 0.1 cm^{-1}. For the high–resolution spectra used in figures 7.6 and 7.7, the spectrum bins were set to 0.005 cm^{-1}. The walks to calculate I(ν,E) were carried out until all of the energy bins (of the total internal vibrational energy) were visited an average of 2,500 times.

7.3.5 Cascade spectra

A total of twenty PAHs were subjected to the simulated cascade method described in this work; seven neutral PAHs and their cationic counterparts: naphthalene,

anthracene, tetracene, phenanthrene, chrysene, pyrene, and benz[a]anthracene; and six aliphatic containing PAHs: 9–methylanthracene, 9,10–dimethylanthracene, 9,10–dihydroanthracene, 9,10–dihydrophenanthrene, 1,2,3,4–tetrahydronaphthalene, and 1,2,3,6,7,8–hexahydropyrene. These molecules were chosen based on previous confirmation of their anharmonic infrared spectra compared with matrix–isolation data, NIST database gas–phase data, as well as high–resolution, mass–selected, low–temperature, gas–phase spectra in our previous work[105, 125, 132]. Four separate simulations were run for each molecule with varying excitation photon energies: 3, 6, 9, and 12 eV. The cascade spectrum of each PAH was simulated using 1×10^7 UV photons, resulting in approximately 1×10^9 emitted IR photons per simulation.

7.4 Results

In order to test the reliability of the Wang–Landau method, Figure 7.6 shows a comparison of the ν_{46} vibrational band of naphthalene between the Wang–Landau approach, the high–resolution experimental data of reference 84, and the direct counting method as described in reference 84. The Wang–Landau method is able to reproduce the spectrum as well as the direct counting method. Differences in band positions between the Wang–Landau and the direct counting method are mainly due to differences in the DFT functional used. Attempts to use the QFF from their online supporting material were made. However, as confirmed by the original authors of reference 84, their QFF was corrected post–calculation and differs from the online version. Therefore, an *exact* one to one comparison between the Wang–Landau and direct counting method was not possible here.

The features in the unconvolved spectrum of Figure 7.6 (blue) are individual peaks (not noise), and each feature can be individually assigned with careful book-keeping during the energy dependent spectrum generation step. Figure 7.7 shows an example of a series of zoomed in panels to show the level of detail that can be achieved even with the random walk. Unlike the direct counting method, no prior cutoff of states to visit (i.e., sufficient thermal population) must be specified. Therefore, the detail becomes limited by the number of Wang–Landau steps taken, and the bin size set, for the energy dependent spectrum generation.

Peak positions of cascade features compared to "0 Kelvin" theoretical anharmonic spectra are found to be equal. While large shifts in peak positions are expected for high temperature/highly excited molecules (equation 7.6), the nature of the IR cascade process leads to features that are not shifted. While the high internal–energy emissions of IR photons are indeed shifted in position, the emission probability is also broadened. This results in the lowering of probability of emitting an IR photon at its "peak" position when compared to lower internal–energy emission, as shown in Figure 7.8. This results in the piling up of IR photons at relatively the same position during lower internal–energy emissions, while the high internal–energy IR photons are spread over a larger area. An increase in initial UV photon energy therefore results *only* in the growth of a low–energy wing, with no change in the position of the peak intensity. The only shifts seen in the resulting

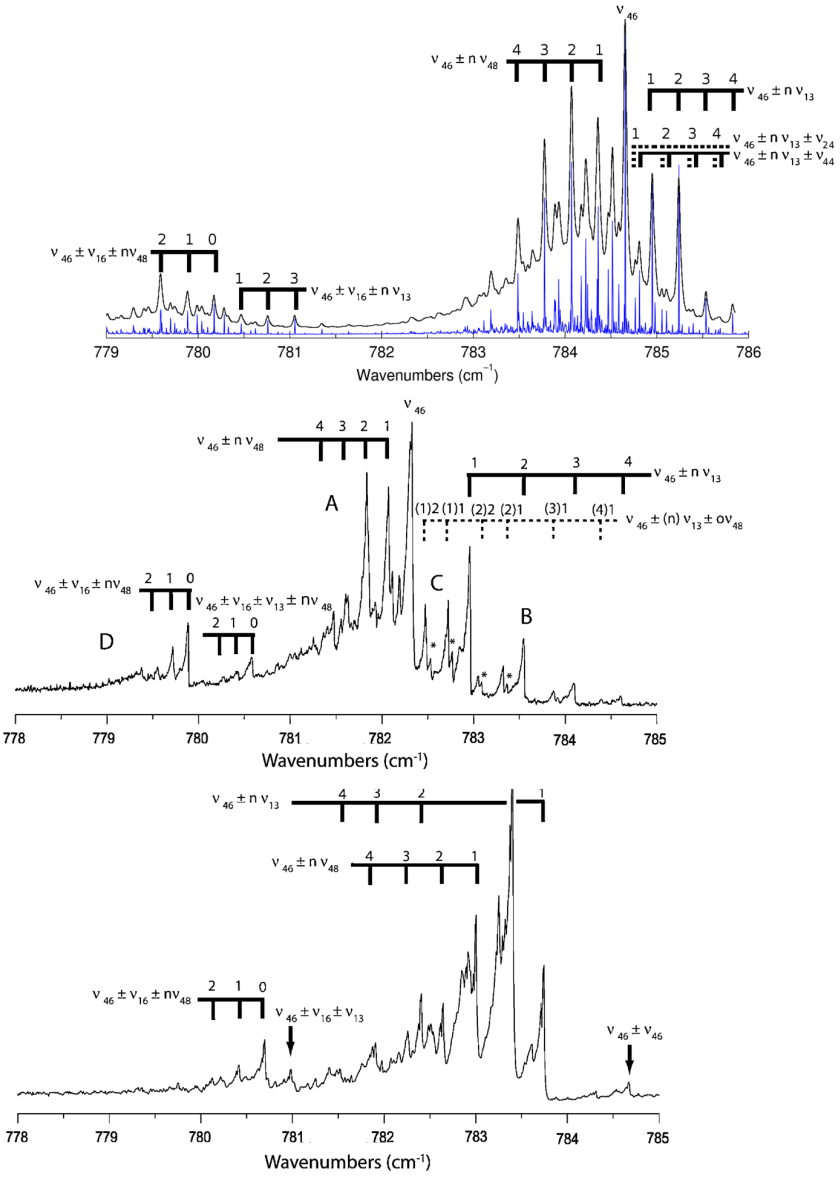

Figure 7.6 Comparison of high–resolution experimental data of thermally excited naphthalene (300 K)[84] (middle panel) to the "direct" theoretical approach[84] (bottom panel) to the Wang–Landau method of this work (top panel, blue, with convolved spectrum in black). Figure has been partially adopted from reference 84.

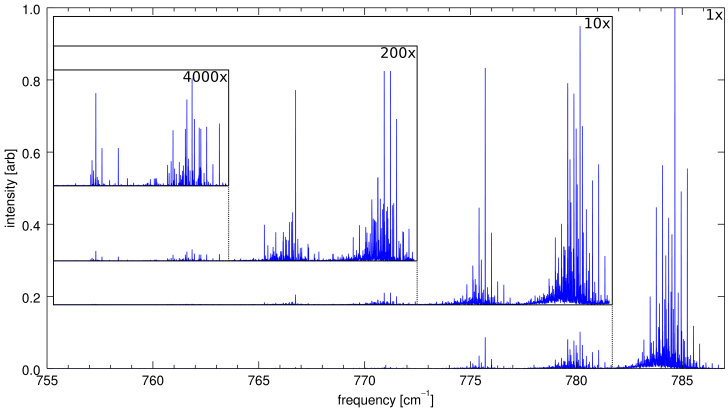

Figure 7.7 A sampling of the series hot–band features of the ν_{46} band of naphthalene at 300 K simulated using the Wang–Landau method for producing a temperature dependent spectrum. Total magnification is given for each portion of the spectrum.

spectra are due to secondary effects as described below. No growth is seen in the high–energy wings, leaving an unchanging steep wall on the high–energy side of the majority of features.

Shifts of the features *appear* to occur, however these "pseudoshifts" are not due to the typical temperature related shifts per se, but are instead due to the cascade process as a whole. The dominant type of pseudoshift occurs when separate IR modes are closely spaced. As the initial exciting UV photon energy is increased, more IR photons are released in an ever growing low–energy IR wing. This lowers the relative peak intensity of all of the cascade features, however, if two or more features are closely spaced then the low–energy IR wing of one feature can slip under the peak of its neighbor, which in turn inhibits the degradation of the neighboring feature. This can cause the lower energy feature to become more intense than the previously stronger higher energy feature (as shown in the bottom panel of Figure 7.9). Even very weak neighboring features can cause the appearance of a shift. The amount of shifting produced by this phenomenon depends on the initial band spacing, and has been observed to occur for bands separated by up to 20 cm^{-1} for cascades starting at high energies. Once the lower intensity neighbor overtakes the initially intense band the "shifting" stops abruptly.

Although the vast majority of cascade features do not appear to move with excitation energies, in rare cases the growth of a high energy wing and shift in feature position can occur in the CH–stretching region for combination bands that are of higher frequency than the fundamentals. This occurs due to Fermi resonances. The magnitude of interaction between resonating modes has been shown to change at different internal energies in the CH–stretching region of some PAHs[141]. Due to

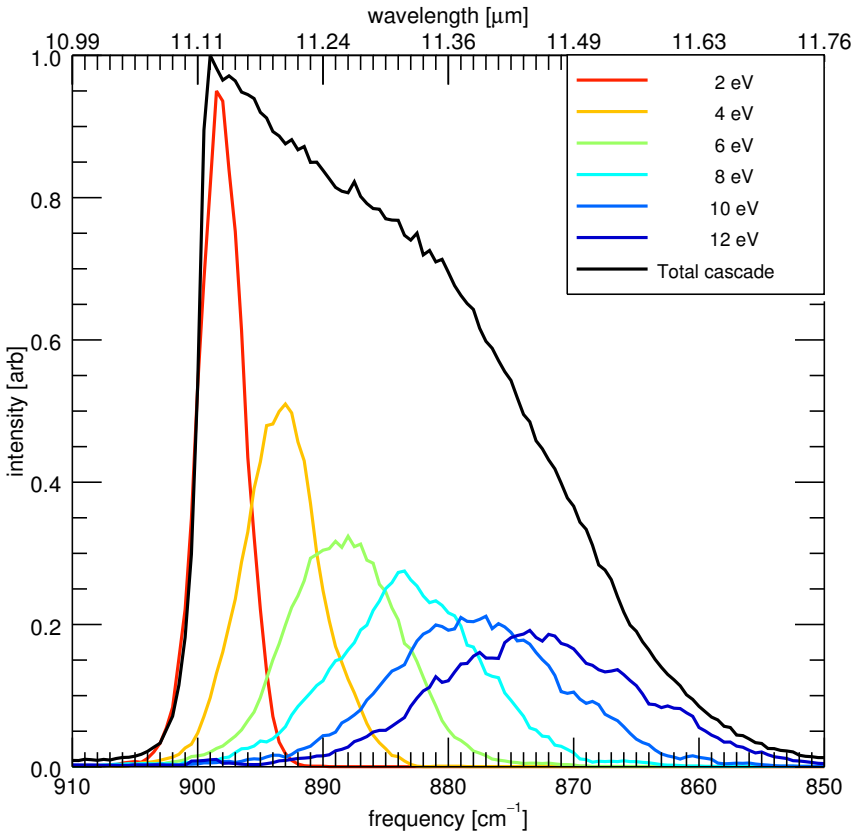

Figure 7.8 The distribution of IR photon emission probabilities at various internal energies along the cascade of a C–H out–of–plane bending mode of tetracene (colors), with the resulting IR cascade spectrum (black).

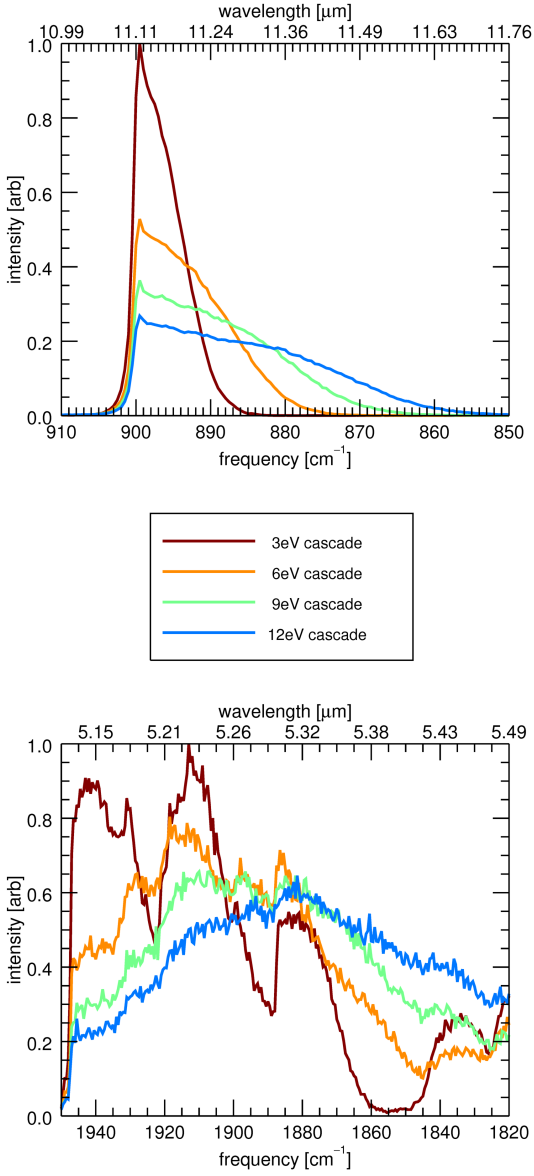

Figure 7.9 Example of the pseudoshifts seen in the theoretical IR cascade spectra at various starting cascade energies. Top: an isolated tetracene band, bottom: closely spaced phenanthrene bands.

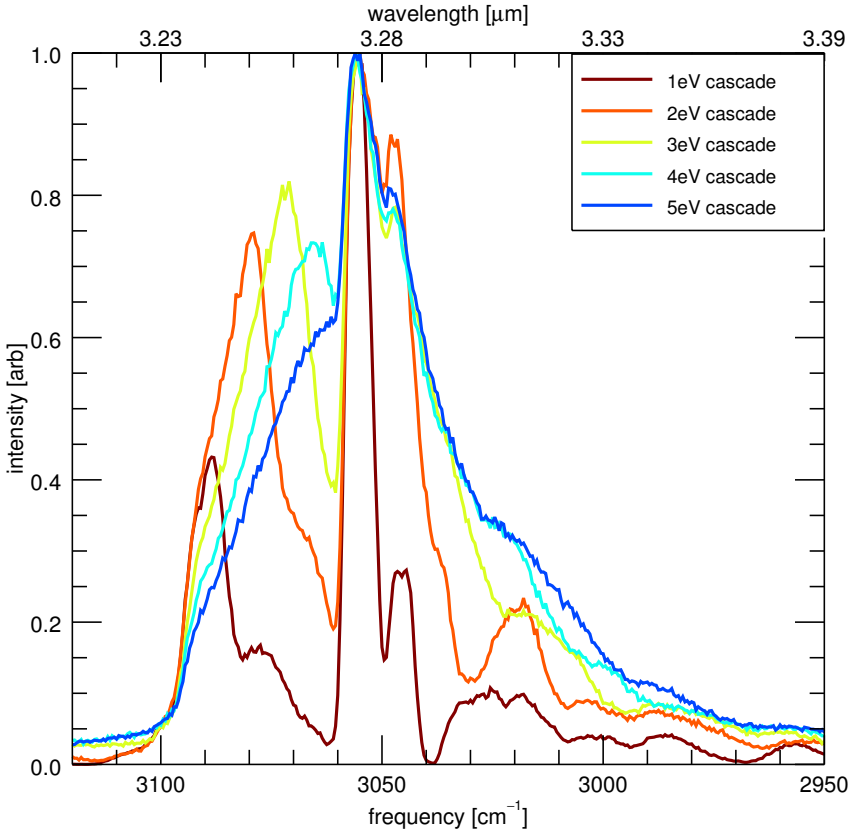

Figure 7.10 The IR cascade spectrum of the CH–stretching region of tetracene.

differences in the anharmonic constants and quantum occupation numbers, fundamental bands and combination bands shift at different rates, leading to resonances that wax and wane as the states move closer and further apart in energy. This results in more intensity being borrowed by the combination bands at particular internal energies. Although minor in most cases, tetracene shows this effect quite strongly (figure 7.10). The feature at 3100 cm^{-1} can be seen to grow and then shrink relative the the strongest band as the cascade starting energy is increased, while the other main features show the typical stationary behavior.

7.5 Conclusions

As shown throughout the theoretical section of this work and in previous studies, careful anharmonic treatment is necessary to reproduce experimental results for PAHs: The inclusion of anharmonicities accounts for the large shifts seen in harmonic fundamental band positions; Fermi resonances dominate the CH–stretching region and account for the large number of bands observed; anharmonic temperature affects account for band shifts and broadenings (and need to be included in the polyad treatments), with the Wang–Landau approach being preferred due to its efficiency, and ease of incorporation of resonances.

It was previously believed that a PAH IR absorption spectrum greatly differs from an IR cascade emission spectrum. Previous cascade emission models[142] of PAHs applied a 15 cm^{-1} shift indiscriminately to all absorption spectra in order to account for the anharmonic emission processes. As this study shows, the experimental shifts observed are due to the pseudoshifts described above rather than anharmonic temperature shifts. Therefore, it will be quite straightforward to transform measured or calculated PAH absorption spectra into cascade spectra relevant for astrophysics as frequency shifts are not relevant.

While this work shows the complexity necessary to reproduce the temperature/energy dependent spectra of PAHs, this work also suggests that this complexity may be unnecessary for the cascade spectra. The stability of the peak positions of the cascade spectra enables the use of 0 Kelvin anharmonic theoretical spectra, or low–temperature gas–phase *absorption* experimental spectra to determine the peak positions (or high energy wall) of IR emission cascade spectra. Previous work has suggested this was not possible[43]. This knowledge can be used to both simplify and improve greatly the current astronomical PAH IR cascade spectra models[36]. To this end, further research into the "growth" rate of the cascade wings as function of initial cascade energy is currently underway.

Acknowledgments

The spectroscopic study of interstellar PAHs at Leiden Observatory have been supported through a Spinoza award, and through the Dutch Astrochemistry Network funded by the Netherlands Organization for Scientific Research, NWO. This work is partly supported by a Royal Netherlands Academy of Arts and Sciences (KNAW) professor prize. We acknowledge the European Union (EU) and Horizon

2020 funding awarded under the Marie Sklodowska–Curie action to the EUROPAH consortium, grant number 722346. Calculations were carried out on the Dutch national e–infrastructure (Cartesius) with the support of SURF Cooperative, under NWO EW project SH-362-15. TC sincerely thanks the support from Swedish Research Council (grant No. 2015-06501). AC acknowledges NWO for a VENI grant (639.041.543). XH and TJL gratefully acknowledge support from the NASA 12–APRA12–0107 grant. XH acknowledges the support from NASA/SETI Co–op Agreement NNX15AF45A. This material is based upon work supported by the National Aeronautics and Space Administration through the NASA Astrobiology Institute under Cooperative Agreement Notice NNH13ZDA017C issued through the Science Mission Directorate.